

Parallel force and position control of flexible manipulators

B. Siciliano and L. Villani

Abstract: The problem of controlling the interaction of a flexible link manipulator with a compliant environment is considered. The manipulator's tip is required to keep contact with a surface by applying a constant force and maintaining a prescribed position or following a desired path on the surface. Using singular perturbation theory, the system is decomposed into a slow subsystem associated with rigid motion and a fast subsystem associated with link flexible dynamics. A parallel force and position control developed for rigid robots is adopted for the slow subsystem while a fast control action is employed to stabilise the link deflections. Simulation results are presented for a two-link planar manipulator under gravity in contact with an elastically compliant surface.

1 Introduction

Lightweight flexible robots are used in a large variety of fields including teleoperation, space robotics, and nuclear waste manipulation. The potential advantages offered by such structures with respect to conventional industrial robots are high speed, large workspace and high payload-to-arm weight [1].

The dynamics of multilink flexible manipulators is, however, much more complex than rigid robot dynamics, due to the distributed flexibility of the links [2]. As a consequence, several challenging problems are still open, regarding both modelling and control aspects.

From the modelling standpoint, the dynamics of a flexible structure is described by infinite dimensional model. Various techniques have been proposed to achieve approximate finite dimensional models (e.g. the assumed modes method, the finite elements method and the Ritz-Kantorovich expansion). In the case of multilink flexible manipulators, a recursive procedure can be set up for dynamic model computation by using a Lagrangian formulation in conjunction with the assumed mode technique [3].

The inherent difficulty of the control problem can be ascribed to the fact that the number of controlled variables is strictly less than the number of mechanical degrees of freedom. Moreover, the dynamic relation between the input torques of the joint actuators and the tip position reveals a behaviour which is the nonlinear counterpart of the nonminimum phase phenomenon of linear systems. Hence, inversion-based control strategies would normally lead to instability in the closed loop. See [4] and the

references therein for further discussion about modelling and control problems for flexible link manipulators.

An effective approach to motion control design is based on singular perturbation theory [5]. When the link stiffness is large, a two-time scale model of the flexible manipulator can be derived [6], consisting in a slow subsystem corresponding to the rigid body motion and a fast subsystem describing the flexible motion. A composite control strategy can be then applied, based on a slow control designed for the equivalent rigid manipulator and a fast control which stabilises the fast subsystem. Further developments of perturbation techniques for flexible manipulators can be found in [7–10].

When the manipulator interacts with an external environment, suitable strategies have to be adopted to control both the tip position and the contact force. While several control schemes have been proposed to force and position control of rigid robot manipulators [11], only few papers on interaction control of flexible manipulators have been published so far.

Early works addressing stability problems in force controlled flexible manipulators are [12, 13]. Models for multilink constrained flexible robots have been developed in [14, 15] where an hybrid position and force control approach is adopted. Hybrid control is used in [16] and [17] to design robust and adaptive control strategies respectively as well as in [18, 19] to control a flexible macro manipulator carrying a rigid micro. In most of these papers ([13, 15, 17]) singular perturbation techniques are exploited to cope with link flexibility; a singular perturbed model for a constrained multilink flexible manipulator was developed in [20].

The singular perturbation method is adopted in this paper to design a force and position control for flexible manipulators based on the parallel approach developed in [21, 22] for rigid robots in contact with compliant environments. As opposed to the hybrid control strategies where force and position are controlled in reciprocal subspaces [23, 24], both force and position variables are used in each subspace without any selection mechanism. This makes parallel controllers suitable to manage contacts with non

© IEE, 2000

IEE Proceedings online no. 20000730

DOI: 10.1049/ip-cta:20000730

Paper first received 17th November 1999 and in revised form 21st June 2000

The authors are with PRISMA Lab, Dipartimento di Informatica e Sistemistica, Università degli Studi di Napoli Federico II, Via Claudio 21, 80125 Napoli, Italy

perfectly known environments and unplanned collisions, which represent a drawback for hybrid controllers. Moreover, differently from previous works tackling the problem of force and position control of flexible manipulators [13, 15, 17, 20], the equations of the constraint environment have not to be taken into account for control design; hence the singular perturbed model for unconstrained robots developed in [6] can be adopted.

Two different parallel control schemes are considered for the slow dynamics; the first ensures force and position regulation, while the second guarantees force regulation and position tracking. An additional control action is required in both cases to stabilise the fast dynamics related to link flexibility.

The proposed control schemes are tested in simulation on the model of a two-link planar manipulator developed in [25]; interaction with an elastically compliant plane is considered. The numerical case study confirms the results anticipated in theory.

2 Modelling

Consider a robot manipulator composed by a serial chain of n flexible links connected by rigid revolute joints subject only to bending deformations in the plane of motion, without torsional effects. A sketch of a two-link manipulator is shown in Fig. 1 with co-ordinate frame assignment. The rigid motion is described by the joint angles ϑ_i , while $w_i(x_i)$ denotes the transversal deflection of link i at x_i with $0 \leq x_i \leq l_i$, being l_i the link length.

A finite-dimensional model (of order m_i) of link flexibility can be obtained by the assumed mode technique [2]. Links are modelled as Euler-Bernoulli beams of uniform density ρ_i and constant flexural rigidity $(EI)_i$, with deflection $w_i(x_i, t)$ satisfying the partial differential equation:

$$(EI)_i \frac{\partial^4 w_i(x_i, t)}{\partial x_i^4} + \rho_i \frac{\partial^2 w_i(x_i, t)}{\partial t^2} = 0, \quad i = 1, \dots, n. \quad (1)$$

Exploiting separability in time and space of solutions of eqn. 1, the link deflection $w_i(x_i, t)$ can be expressed as the sum of a finite number of modes:

$$w_i(x_i, t) = \sum_{j=1}^{m_i} \phi_{ij}(x_i) \delta_{ij}(t) \quad (2)$$

where $\phi_{ij}(x)$ is the shape assumed for the j th mode of link i , and $\delta_{ij}(t)$ is its time-varying amplitude. The mode shapes have to satisfy proper boundary conditions at the base (clamped) and at the end of each link (mass).

In view of eqn. 2, a direct kinematics equation can be derived expressing the (2×1) position vector \mathbf{p} of the manipulator tip point as a function of the $(n \times 1)$ joint

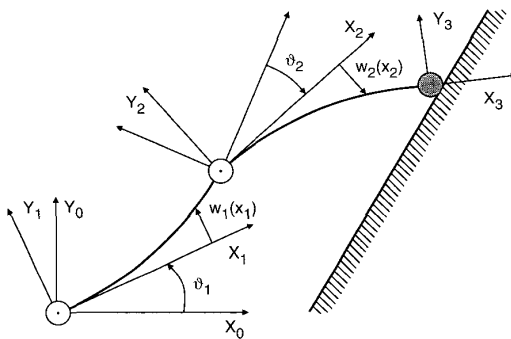


Fig. 1 Planar two-link flexible manipulator

variable vector $\boldsymbol{\vartheta} = [\vartheta_1 \dots \vartheta_n]^T$ and the $(m \times 1)$ deflection variable vector $\boldsymbol{\delta} = [\delta_{11} \dots \delta_{1m_1} \dots \delta_{n1} \dots \delta_{nm_n}]^T$ [3, 25], i.e.

$$\mathbf{p} = \mathbf{k}(\boldsymbol{\vartheta}, \boldsymbol{\delta}) \quad (3)$$

In view of eqn. 3, the differential kinematics equation expressing the tip velocity $\dot{\mathbf{p}}$ as a function of $\boldsymbol{\vartheta}$ and $\boldsymbol{\delta}$, can be written in the form:

$$\dot{\mathbf{p}} = \mathbf{J}_\vartheta(\boldsymbol{\vartheta}, \boldsymbol{\delta}) \dot{\boldsymbol{\vartheta}} + \mathbf{J}_\delta(\boldsymbol{\vartheta}, \boldsymbol{\delta}) \dot{\boldsymbol{\delta}} \quad (4)$$

where $\mathbf{J}_\vartheta = \partial \mathbf{k} / \partial \boldsymbol{\vartheta}$ and $\mathbf{J}_\delta = \partial \mathbf{k} / \partial \boldsymbol{\delta}$.

Assume that the manipulator is in contact with the environment. By virtue of the virtual work principle, the vector \mathbf{f} of the forces exerted by the manipulator on the environment performing work on \mathbf{p} has to be related to the $(n \times 1)$ vector $\mathbf{J}_\vartheta^T \mathbf{f}$ of joint torques performing work on $\boldsymbol{\vartheta}$ and the $(m \times 1)$ vector $\mathbf{J}_\delta^T \mathbf{f}$ of the elastic reaction forces performing work on $\boldsymbol{\delta}$.

Using the assumed modes link approximation (eqn. 2), a finite-dimensional Lagrangian dynamic model of the planar manipulator in contact with the environment can be obtained as a function of the $n + m$ vector of generalised coordinates $\mathbf{q} = [\boldsymbol{\vartheta}^T \boldsymbol{\delta}^T]^T$ in the form [3, 25],

$$\mathbf{B}(\mathbf{q}) \ddot{\mathbf{q}} + \mathbf{c}(\mathbf{q}, \dot{\mathbf{q}}) + \mathbf{g}(\mathbf{q}) + \begin{bmatrix} 0 \\ \mathbf{D} \dot{\boldsymbol{\delta}} + \mathbf{K} \boldsymbol{\delta} \end{bmatrix} = \begin{bmatrix} \boldsymbol{\tau} \\ 0 \end{bmatrix} - \mathbf{J}^T(\mathbf{q}) \mathbf{f} \quad (5)$$

where \mathbf{B} is the positive definite symmetric inertia matrix, \mathbf{c} is the vector of Coriolis and centrifugal torques, \mathbf{g} is the vector of gravitational torques, \mathbf{K} is the diagonal and positive definite link stiffness matrix, \mathbf{D} is the diagonal and positive semidefinite link damping matrix, $\boldsymbol{\tau}$ is the vector of the input joint torques and $\mathbf{J}(\mathbf{q}) = [\mathbf{J}_\vartheta(\mathbf{q}) \mathbf{J}_\delta(\mathbf{q})]$ is the manipulator Jacobian.

By partitioning the matrix and vectors in blocks according to the rigid and flexible components, the equation of motion (eqn. 5) can be rewritten as:

$$\begin{bmatrix} \mathbf{B}_{\vartheta\vartheta}(\boldsymbol{\vartheta}, \boldsymbol{\delta}) & \mathbf{B}_{\vartheta\delta}(\boldsymbol{\vartheta}, \boldsymbol{\delta}) \\ \mathbf{B}_{\delta\vartheta}^T(\boldsymbol{\vartheta}, \boldsymbol{\delta}) & \mathbf{B}_{\delta\delta}(\boldsymbol{\vartheta}, \boldsymbol{\delta}) \end{bmatrix} \begin{bmatrix} \dot{\boldsymbol{\vartheta}} \\ \dot{\boldsymbol{\delta}} \end{bmatrix} + \begin{bmatrix} \mathbf{c}_\vartheta(\boldsymbol{\vartheta}, \boldsymbol{\delta}, \dot{\boldsymbol{\vartheta}}, \dot{\boldsymbol{\delta}}) \\ \mathbf{c}_\delta(\boldsymbol{\vartheta}, \boldsymbol{\delta}, \dot{\boldsymbol{\vartheta}}, \dot{\boldsymbol{\delta}}) \end{bmatrix} + \begin{bmatrix} \mathbf{g}_\vartheta(\boldsymbol{\vartheta}, \boldsymbol{\delta}) \\ \mathbf{g}_\delta(\boldsymbol{\vartheta}, \boldsymbol{\delta}) \end{bmatrix} + \begin{bmatrix} 0 \\ \mathbf{D} \dot{\boldsymbol{\delta}} + \mathbf{K} \boldsymbol{\delta} \end{bmatrix} = \begin{bmatrix} \boldsymbol{\tau} \\ 0 \end{bmatrix} - \begin{bmatrix} \mathbf{J}_\vartheta^T(\boldsymbol{\vartheta}, \boldsymbol{\delta}) \mathbf{f} \\ \mathbf{J}_\delta^T(\boldsymbol{\vartheta}, \boldsymbol{\delta}) \mathbf{f} \end{bmatrix} \quad (6)$$

3 Two-time scale control

When the link stiffness is large, it is reasonable to expect that the dynamics related to link flexibility is much faster than the dynamics associated with the rigid motion of the robot so that the system naturally exhibits a two-time scale dynamic behaviour in terms of rigid and flexible variables. This feature can be conveniently exploited for control design.

Following the approach proposed in [6], the system can be decomposed in a slow and a fast subsystems by using singular perturbation theory; this leads to a composite control strategy for the full system based on separate control designs for the two reduced-order subsystems.

Assuming that full-state measurement is available and that a force sensor is mounted at the manipulator tip, the joint torques can be conveniently chosen as:

$$\boldsymbol{\tau} = \mathbf{g}_\vartheta(\boldsymbol{\vartheta}, \boldsymbol{\delta}) + \mathbf{J}_\vartheta(\boldsymbol{\vartheta}, \boldsymbol{\delta})^T \mathbf{f} + \mathbf{u} \quad (7)$$

in order to cancel out the effects of the static torques acting on the rigid part of the manipulator dynamics; the vector \mathbf{u} is the new control input to be designed on the basis of the singular perturbation approach.

The time scale separation between the slow and fast dynamics can be determined by defining the singular perturbation parameter $\epsilon = 1/\sqrt{(k_m)}$, where k_m is the smallest coefficient of the diagonal stiffness matrix \mathbf{K} , and the new variable:

$$\mathbf{z} = \mathbf{K}\delta = \frac{1}{\epsilon^2}\hat{\mathbf{K}}\delta \quad (8)$$

corresponds to the elastic force, where $\mathbf{K} = k_m\hat{\mathbf{K}}$. Considering the inverse \mathbf{H} of the inertia matrix \mathbf{B} , the dynamic model (eqn. 6), with control law (eqn. 7), can be rewritten in terms of the new variable \mathbf{z} as:

$$\begin{aligned} \ddot{\boldsymbol{\theta}} &= \mathbf{H}_{\theta\theta}(\boldsymbol{\theta}, \epsilon^2\mathbf{z})(\mathbf{u} - \mathbf{c}_\theta(\boldsymbol{\theta}, \epsilon^2\mathbf{z}, \dot{\boldsymbol{\theta}}, \epsilon^2\dot{\mathbf{z}})) \\ &\quad - \mathbf{H}_{\theta\delta}(\boldsymbol{\theta}, \epsilon^2\mathbf{z})(\mathbf{c}_\delta(\boldsymbol{\theta}, \epsilon^2\mathbf{z}, \dot{\boldsymbol{\theta}}, \epsilon^2\dot{\mathbf{z}}) + \mathbf{g}_\delta(\boldsymbol{\theta}, \delta)) \\ &\quad + \epsilon^2\mathbf{D}\hat{\mathbf{K}}^{-1}\dot{\mathbf{z}} + \mathbf{z} + \mathbf{J}_\delta^T(\boldsymbol{\theta}, \delta)\mathbf{f} \end{aligned} \quad (9)$$

$$\begin{aligned} \epsilon^2\ddot{\mathbf{z}} &= \hat{\mathbf{K}}\mathbf{H}_{\delta\delta}^T(\boldsymbol{\theta}, \epsilon^2\mathbf{z})(\mathbf{u} - \mathbf{c}_\theta(\boldsymbol{\theta}, \epsilon^2\mathbf{z}, \dot{\boldsymbol{\theta}}, \epsilon^2\dot{\mathbf{z}})) \\ &\quad - \hat{\mathbf{K}}\mathbf{H}_{\delta\delta}(\boldsymbol{\theta}, \epsilon^2\mathbf{z})(\mathbf{c}_\delta(\boldsymbol{\theta}, \epsilon^2\mathbf{z}, \dot{\boldsymbol{\theta}}, \epsilon^2\dot{\mathbf{z}}) + \mathbf{g}_\delta(\boldsymbol{\theta}, \delta)) \\ &\quad + \epsilon^2\mathbf{D}\hat{\mathbf{K}}^{-1}\dot{\mathbf{z}} + \mathbf{z} + \mathbf{J}_\delta^T(\boldsymbol{\theta}, \delta)\mathbf{f} \end{aligned} \quad (10)$$

where a suitable partition of \mathbf{H} has been considered:

$$\mathbf{H} = \mathbf{B}^{-1} = \begin{bmatrix} \mathbf{H}_{\theta\theta} & \mathbf{H}_{\theta\delta} \\ \mathbf{H}_{\theta\delta}^T & \mathbf{H}_{\delta\delta} \end{bmatrix} \quad (11)$$

Eqns. 9 and 10 represent a singularly perturbed form of the flexible manipulator model; when $\epsilon \rightarrow 0$, the model of an equivalent rigid manipulator is recovered. In fact, setting $\epsilon = 0$ and solving for \mathbf{z} in eqn. 10 gives:

$$\begin{aligned} \mathbf{z}_s &= \bar{\mathbf{H}}_{\delta\delta}^{-1}(\boldsymbol{\theta}_s)\bar{\mathbf{H}}_{\theta\delta}^T(\boldsymbol{\theta}_s)(\mathbf{u}_s - \bar{\mathbf{c}}_\theta(\boldsymbol{\theta}_s, \dot{\boldsymbol{\theta}}_s)) \\ &\quad - \bar{\mathbf{c}}_\delta(\boldsymbol{\theta}_s, \dot{\boldsymbol{\theta}}_s) - \bar{\mathbf{g}}_\delta(\boldsymbol{\theta}_s) - \bar{\mathbf{J}}_\delta^T(\boldsymbol{\theta}_s)\mathbf{f}_s \end{aligned} \quad (12)$$

where the subscript s indicates that the system is considered in the slow time scale and the overbar denotes that a quantity is computed with $\epsilon = 0$. Plugging eqn. 12 into eqn. 9 with $\epsilon = 0$ yields:

$$\ddot{\boldsymbol{\theta}}_s = \bar{\mathbf{B}}_{\theta\theta}^{-1}(\boldsymbol{\theta}_s)(\mathbf{u}_s - \bar{\mathbf{c}}_\theta(\boldsymbol{\theta}_s, \dot{\boldsymbol{\theta}}_s)) \quad (13)$$

where the equality:

$$\bar{\mathbf{B}}_{\theta\theta}^{-1}(\boldsymbol{\theta}_s) = (\bar{\mathbf{H}}_{\theta\theta}(\boldsymbol{\theta}_s) - \bar{\mathbf{H}}_{\theta\delta}(\boldsymbol{\theta}_s)\bar{\mathbf{H}}_{\delta\delta}^{-1}(\boldsymbol{\theta}_s)\bar{\mathbf{H}}_{\theta\delta}^T(\boldsymbol{\theta}_s))^{-1} \quad (14)$$

has been exploited, being $\bar{\mathbf{B}}_{\theta\theta}(\boldsymbol{\theta}_s)$ the inertia matrix of the equivalent rigid manipulator and $\bar{\mathbf{c}}_\theta(\boldsymbol{\theta}_s, \dot{\boldsymbol{\theta}}_s)$ the vector of the corresponding Coriolis and centrifugal torques.

The dynamics of the system in the fast time scale can be obtained by setting $t_f = t/\epsilon$, treating the slow variables as constants in the fast time scale, and introducing the fast variables $\mathbf{z}_f = \mathbf{z} - \mathbf{z}_s$; thus, the fast system of eqn. 10 is:

$$\frac{d^2\mathbf{z}_f}{dt_f^2} = -\hat{\mathbf{K}}\bar{\mathbf{H}}_{\delta\delta}(\boldsymbol{\theta}_s)\mathbf{z}_f + \hat{\mathbf{K}}\bar{\mathbf{H}}_{\theta\delta}^T(\boldsymbol{\theta}_s)\mathbf{u}_f \quad (15)$$

where the fast control $\mathbf{u}_f = \mathbf{u} - \mathbf{u}_s$ has been introduced accordingly.

On the basis of the above two-time scale model, the design of a feedback controller for the system (eqns. 9 and

10) can be performed according to a composite control strategy, i.e.

$$\mathbf{u} = \mathbf{u}_s(\boldsymbol{\theta}_s, \dot{\boldsymbol{\theta}}_s) + \mathbf{u}_f(\mathbf{z}_f, d\mathbf{z}_f/dt_f) \quad (16)$$

with the constraint that $\mathbf{u}_f(0, 0) = 0$, so that \mathbf{u}_f is inactive along the equilibrium manifold specified by eqn. 12.

To design the slow control for the rigid nonlinear system (eqn. 13), it is useful to derive the slow dynamics corresponding to the tip position. Differentiating eqn. 4 gives the tip acceleration:

$$\ddot{\mathbf{p}} = \mathbf{J}_\theta(\boldsymbol{\theta}, \delta)\ddot{\boldsymbol{\theta}} + \mathbf{J}_\delta(\boldsymbol{\theta}, \delta)\ddot{\delta} + \mathbf{h}(\boldsymbol{\theta}, \delta, \dot{\boldsymbol{\theta}}, \dot{\delta}) \quad (17)$$

where $\mathbf{h} = \dot{\mathbf{J}}_\theta\boldsymbol{\theta} + \dot{\mathbf{J}}_\delta\delta$; hence the corresponding slow system is:

$$\ddot{\mathbf{p}}_s = \bar{\mathbf{J}}_\theta(\boldsymbol{\theta}_s)\bar{\mathbf{B}}_{\theta\theta}^{-1}(\boldsymbol{\theta}_s)(\mathbf{u}_s - \bar{\mathbf{c}}_\theta(\boldsymbol{\theta}_s, \dot{\boldsymbol{\theta}}_s)) + \bar{\mathbf{h}}(\boldsymbol{\theta}_s, \dot{\boldsymbol{\theta}}_s) \quad (18)$$

where eqn. 13 has been used. The slow dynamic models (eqns. 13 and 18) enjoy the same notable properties of the rigid robot dynamic models [4], hence the control strategies used for rigid manipulators can be adopted.

As for the fast system (eqn. 15), this is a marginally stable linear slowly time-varying system that can be stabilized to the equilibrium manifold $\dot{\mathbf{z}}_f = 0$ ($\dot{\mathbf{z}} = 0$) and $\mathbf{z}_f = 0$ ($\mathbf{z} = \mathbf{z}_s$) by a proper choice of the control input \mathbf{u}_f . A reasonable way to achieve this goal is to design a state-space control law of the form:

$$\mathbf{u}_f = \mathbf{K}_1\dot{\mathbf{z}}_f + \mathbf{K}_2\mathbf{z}_f \quad (19)$$

where, in principle, the matrices \mathbf{K}_1 and \mathbf{K}_2 should be tuned for every configuration $\boldsymbol{\theta}_s$. However, the computational burden necessary to perform this strategy can be avoided by using constant matrix gains tuned with reference to a given robot configuration [6]; any state-space technique can be used, (e.g. based on classical pole placement algorithms).

4 Force and position regulation

The control objective consists in simultaneous regulation of the contact force \mathbf{f} to a constant set point \mathbf{f}_d and of the position \mathbf{p} to a constant set-point \mathbf{p}_d .

In case of contact with an elastically compliant surface, a viable strategy is the parallel control approach [21], which is especially effective in the case of inaccurate contact modeling. The key feature is to have a force control loop working in parallel to a position control loop along each task space direction. The logical conflict between the two loops is managed by imposing dominance of the force control action over the position one, (i.e. force regulation is always guaranteed at the expense of a position error along the constrained directions).

A force/position parallel regulator controller for rigid robots was proposed in [22], based on position PD position control + gravity compensation + desired force feedforward + PI force control.

For the case of the flexible link manipulator (eqn. 5), with reference to the slow system (eqn. 18), the following parallel regulator can be adopted:

$$\mathbf{u}_s = \bar{\mathbf{J}}_\theta^T(\boldsymbol{\theta}_s)k_p(\mathbf{p}_r - \mathbf{p}_s) - k_D\dot{\boldsymbol{\theta}}_s \quad (20)$$

where \mathbf{p}_r is defined as:

$$\mathbf{p}_r = \mathbf{p}_d + k_p^{-1} \left(k_F(\mathbf{f}_d - \mathbf{f}_s) + k_I \int_0^t (\mathbf{f}_d - \mathbf{f}_s) d\tau \right) \quad (21)$$

and $k_p, k_D, k_F, k_I > 0$ are suitable feedback gains.

A better insight into the behaviour of the system during the interaction can be achieved by considering a model of the compliant environment. To this purpose, a planar surface is considered, which is locally a good approximation to surfaces of regular curvature, and a frame with rotation matrix:

$$R_c = \begin{bmatrix} t & n \end{bmatrix} \quad (22)$$

is conveniently chosen with n normal and t tangential to the plane. Thus, the model of the contact force is given by:

$$f = k_e n n^T (p - p_o) \quad (23)$$

where p_o represents the position of any point on the undeformed plane and $k_e > 0$ is the contact stiffness coefficient. For the purpose of this work, it is assumed that the same equation can be established in terms of the slow variables, i.e.

$$f_s = k_e n n^T (p_s - p_o) \quad (24)$$

The above elastic model shows that the contact force is normal to the plane, and thus a null force error can be obtained only if the desired force f_d is aligned with n . Also, it can be recognised that null position errors can be obtained only on the contact plane while the component of the position along n has to accommodate the force requirement specified by f_d .

The stability analysis for the slow system (eqn. 18) with the control law (eqns. 20 and 21) can be carried out with the same arguments used in [22] for the case of rigid robots. In particular, it can be shown that, if the Jacobian $\bar{J}_g(\vartheta_s)$ of the equivalent rigid manipulator is full-rank, the closed loop system has an exponentially stable equilibrium at:

$$p_{s,\infty} = (I - n n^T) p_d + n n^T (k_e^{-1} f_d + p_o) \quad (25)$$

$$f_{s,\infty} = k_e n n^T (p_{s,\infty} - p_o) = f_d \quad (26)$$

where the matrix $(I - n n^T)$ projects the vectors on the contact plane.

The equilibrium position is depicted in Fig. 2. It can be recognised that $p_{s,\infty}$ differs from p_d by a vector aligned along the normal to the contact plane whose magnitude is that necessary to guarantee $f_{s,\infty} = f_d$ in view of (eqn. 26). Therefore (for the slow system) force regulation is ensured, while a null position error is achieved only for the component parallel to the contact plane.

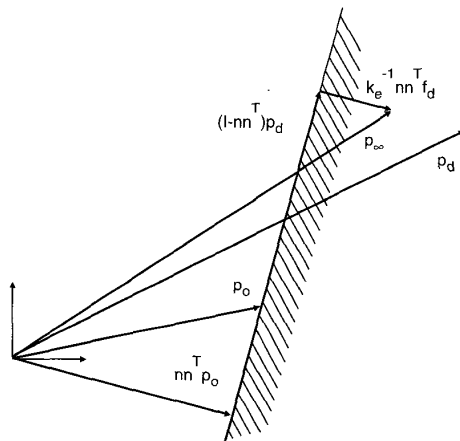


Fig. 2 Equilibrium position with parallel force and position control

If f_d is not aligned with n , it can be found that a drift motion of the manipulator tip is generated along the plane; for this reason, if the contact geometry is unknown, it is advisable to set $f_d = 0$.

As a final step, the full-order system (eqn. 5) and the composite control law (eqn. 16) with u_s in eqn. 20 and u_f in eqn. 19 have to be analysed. By virtue of Tikhonov's theorem, it can be shown that regulation of the force f and of the position p is achieved with an order ϵ approximation.

5 Force regulation and position tracking

The above control scheme provides regulation of the component of the tip position on the contact plane. On the other hand, if tracking of a time-varying position $p_d(t)$ on the contact plane is desired (with an order ϵ approximation), an inverse dynamics parallel control scheme can be adopted for the slow system, i.e.

$$u_s = \bar{B}_{g,\vartheta}(\vartheta_s) \bar{J}_g^{-1}(\vartheta_s) (a_s - \bar{h}(\vartheta_s, \dot{\vartheta}_s)) + \bar{c}_g(\vartheta_s, \dot{\vartheta}_s) \quad (27)$$

where a_s is a new control input and a non-redundant manipulator has been considered. Folding eqn. 27 into eqn. 18 gives:

$$\ddot{p}_s = a_s \quad (28)$$

hence the control input a_s can be chosen as:

$$a_s = \ddot{p}_r + k_D(\dot{p}_r - \dot{p}_s) + k_p(p_r - p_s) \quad (29)$$

where

$$p_r = p_d + p_c \quad (30)$$

and p_c is the solution of the differential equation:

$$k_A \ddot{p}_c + k_V \dot{p}_c = f_d - f_s \quad (31)$$

$k_p, k_D, k_A, k_V > 0$ are suitable feedback gains.

By using for the slow system the same arguments developed in [11] for rigid robots, it can be easily shown that the control law (eqn. 27), (eqns 29–31) ensures regulation of the contact force to the desired set-point f_d and tracking of the time-varying component of the desired position on the contact plane $(I - n n^T) p_d(t)$.

As before, Tikhonov's theorem has to be applied to the full-order system (eqn. 5) with the composite control law (eqns. 16, 27, 29–31 and 19); it can be shown that force regulation and position tracking are achieved with an order ϵ approximation.

6 Simulation

To illustrate the effectiveness of the proposed strategy, a planar two-link flexible manipulator (Fig. 1) is considered:

$$\vartheta = [\vartheta_1 \quad \vartheta_2]^T$$

and an expansion with two clamped-mass assumed modes is taken for each link:

$$\delta = [\delta_{11} \quad \delta_{12} \quad \delta_{21} \quad \delta_{22}]^T$$

The following parameters are set up for the links and a payload is assumed to be placed at the manipulator tip:

$$\rho_1 = \rho_2 = 1.0 \text{ kg/m (link uniform density)}$$

$$\ell_1 = \ell_2 = 0.5 \text{ m (link length)}$$

$$d_1 = d_2 = 0.25 \text{ m (link center of mass)}$$

$$m_1 = m_2 = 0.5 \text{ m (link mass)}$$

$$m_{h1} = m_{h2} = 1 \text{ kg (hub mass)}$$

$$m_p = 0.1 \text{ kg (payload mass)}$$

$(EI)_1 = (EI)_2 = 10 \text{ N m}^2$ (flexural link rigidity).

The stiffness coefficients of the diagonal matrix K are:

$$k_{11} = 38.79 \text{ N} \quad k_{12} = 513.37 \text{ N}$$

$$k_{21} = 536.09 \text{ N} \quad k_{22} = 20792.09 \text{ N}$$

The dynamic model of the manipulator and the missing numerical data can be found in [25], while the direct and differential kinematics equations are reported in [26].

The contact surface is a vertical plane, thus the normal vector in eqn. 23 is $\mathbf{n} = [1 \ 0]^T$; a point of the undeformed plane is:

$$\mathbf{p}_o = [0.55 \ 0]^T \text{ m}$$

and the contact stiffness is $k_e = 50 \text{ N/m}$

The manipulator was initially placed with the tip in contact with the undeformed plane in the position:

$$\mathbf{p}(0) = [0.55 \ -0.55]^T \text{ m}$$

with null contact force; the corresponding generalised coordinates of the manipulator are:

$$\boldsymbol{\vartheta} = [-1.396 \ 1.462]^T \text{ rad}$$

$$\boldsymbol{\delta} = [-0.106 \ 0.001 \ -0.009 \ -0.0001]^T \text{ m}$$

It is desired to reach the tip position:

$$\mathbf{p}_d = [0.55 \ -0.35]^T \text{ m}$$

and a fifth-order polynomial trajectory with null initial and final velocity and acceleration is imposed from the initial to the final position with a duration of 5 s.

The desired force is taken from zero to the desired value:

$$\mathbf{f}_d = [5 \ 0]^T \text{ N}$$

according to a fifth-order polynomial trajectory with null initial and final first and second derivative and a duration of 1 s.

The fast control law \mathbf{u}_f has been implemented with $\epsilon = 0.1606$. The matrix gains in eqn. 19 have been tuned by solving an LQ problem for the system (eqn. 15) with the configuration dependent terms computed in the initial manipulator configuration. The matrix weights of the index performance have been chosen so that to preserve the time-scale separation between slow and fast dynamics for both the control schemes. The resulting matrix gains are:

$$\mathbf{K}_1 = \begin{bmatrix} -0.0372 & -0.0204 & -0.0375 & 0.1495 \\ 0.0573 & 0.0903 & 0.0080 & -0.7856 \end{bmatrix}$$

$$\mathbf{K}_2 = \begin{bmatrix} -0.1033 & -0.0132 & -0.0059 & -0.0053 \\ -0.0882 & 0.0327 & -0.0537 & -0.0217 \end{bmatrix}$$

Numerical simulations have been performed via MATLAB with SIMULINK. In order to reproduce a real situation of a continuous-time system with a digital controller; the control laws are discretised with 5 ms sampling time, while the equations of motion are integrated using a variable step Runge-Kutta method with a minimum step size of 1 ms.

In the first case study, the slow controller (eqns. 20 and 21) has been used in the composite control law (eqn. 16). The actual force \mathbf{f} and position \mathbf{p} are used in the slow

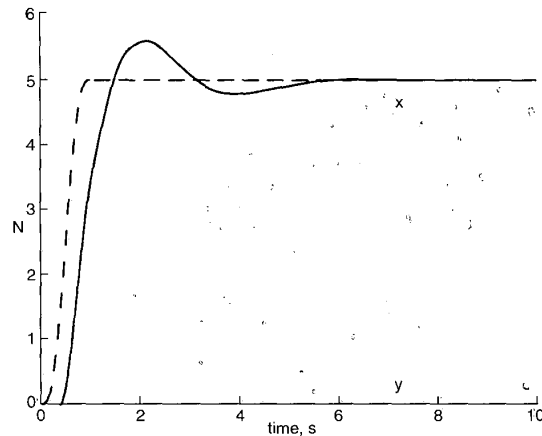


Fig. 3 Time history of contact force in first case study

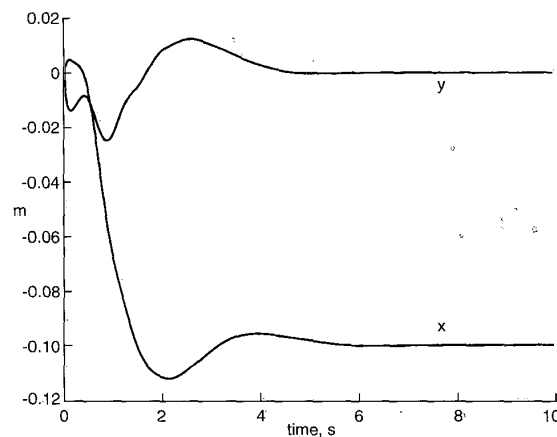


Fig. 4 Time history of position error in first case study

control law instead of the corresponding slow values, assuming that direct force measurement is available and that the tip position is computed from joint angles and link deflection measurements *via* the direct kinematics (eqn. 3). The control gains have been set to $k_P = 100$, $k_D = 4$, $k_F = 100$, $k_I = 500$.

In Fig. 3 the time histories of the desired (dashed) and actual (solid) contact force are reported, together with the position error in Fig. 4. It is easy to see that the contact force remains close to the desired value during the tip motion (notice that the commanded position trajectory has a 5 s duration) and reaches the desired set-point at steady state. Only the y -component of the desired position is regulated to the desired value, while a significant error occurs for the x -component; its (constant) value at steady state is exactly that required to achieve null force error along the same axis, according to the equilibrium eqns. 25 and 26.

The time histories of the joint angles and link deflections are reported in Figs. 5–8. It can be recognised that the oscillations of the link deflections are well damped; moreover, because of gravity and contact force, the manipulator has to bend to reach the desired tip position with the desired contact force.

Figs. 9 and 10 show the time history of the joint torque \mathbf{u} and the first 0.5 s of the time history of the fast torque \mathbf{u}_f . It can be observed that the control effort keeps

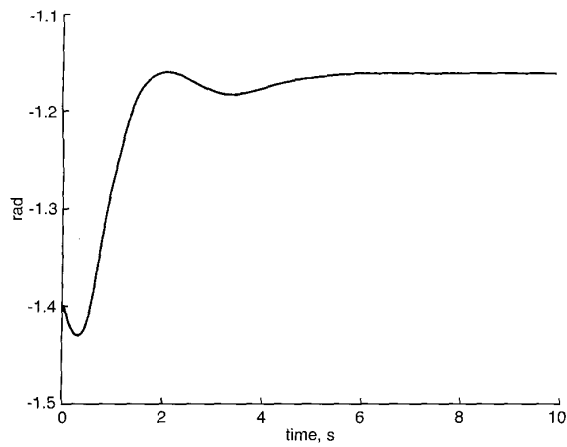


Fig. 5 Time history of first joint angle in first case study

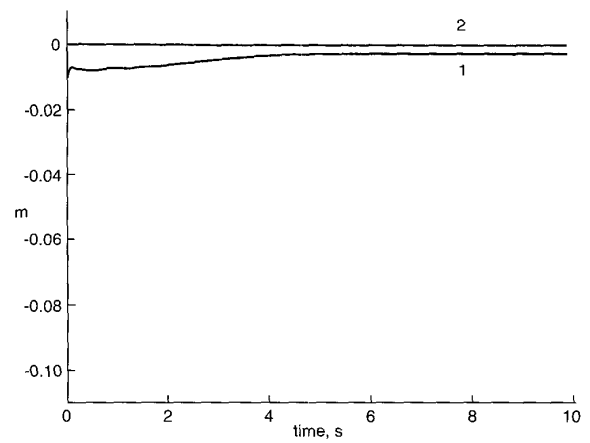


Fig. 8 Time histories of second link deflections in first case study

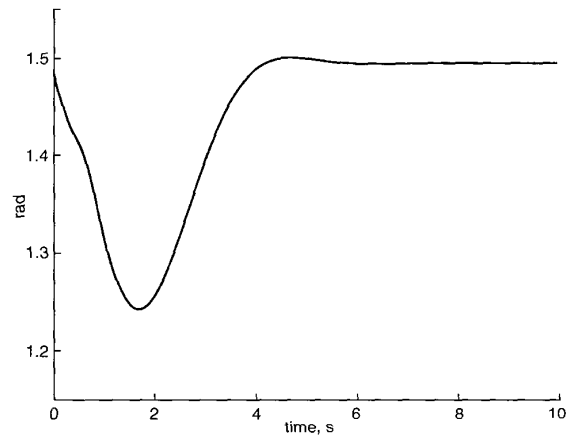


Fig. 6 Time history of second joint angle in first case study

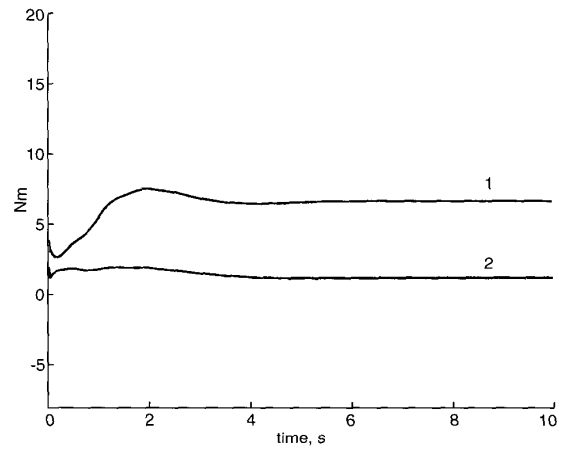


Fig. 9 Time histories of joint torques in first case study

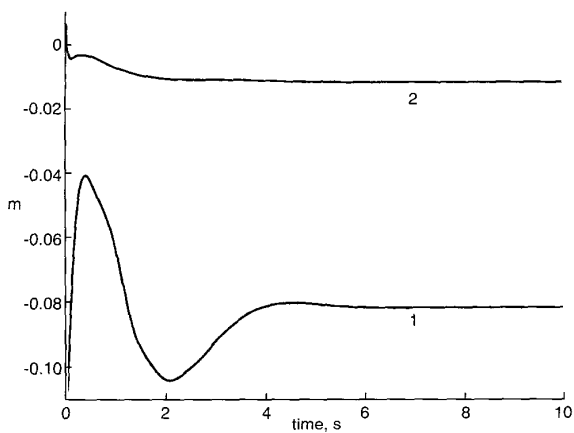


Fig. 7 Time histories of first link deflections in first case study

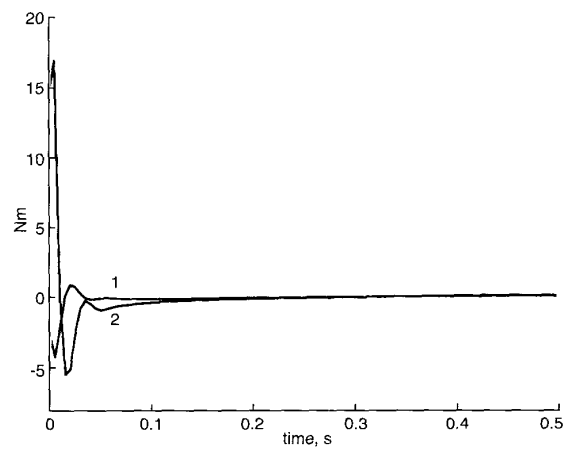


Fig. 10 Time history of fast control in first case study

limited values during task execution; remarkably, the control torque u_f converges to zero with a transient much faster than the transient of u , as expected.

In the second case study, the slow controller (eqns. 27, 29–31) has been used in the composite control law (eqn. 16). As before, the actual force f and position p are used in the controller in lieu of the corresponding slow variables. The control gains have been set to $k_p = 100$, $k_D = 22$, $k_A = 0.7813$, $k_V = 13.75$.

In Figs. 11 and 12 the time histories of the contact force and position errors are reported. This time the desired force

set-point is reached after about 3 s, before the completion of the tip motion; moreover, the tracking performance for the the y -component of the desired position is better than in the previous case study.

The time histories of the joint angles and of the link deflections are reported in Figs. 13–16, while the time histories of the components of the joint torque vector u and of the fast torque vector u_f are reported in Figs. 17 and 18. It can be recognised that, although the performance is better than in the previous case study, a similar control effort is required.

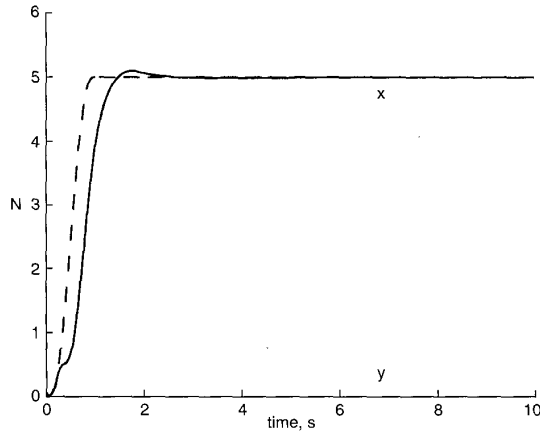


Fig. 11 Time history of contact force in second case study

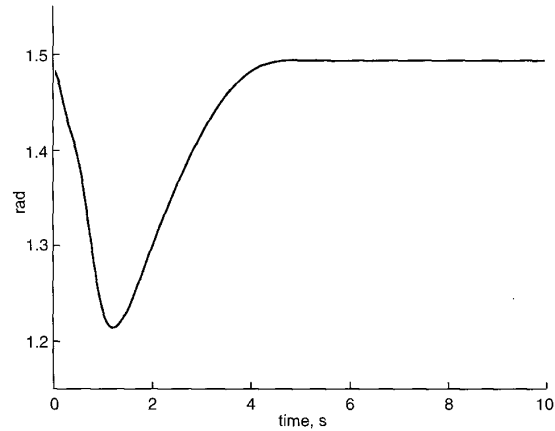


Fig. 14 Time history of second joint angle in second case study

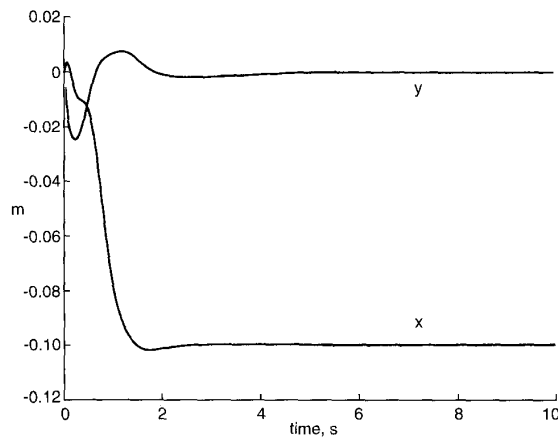


Fig. 12 Time history of position error in second case study

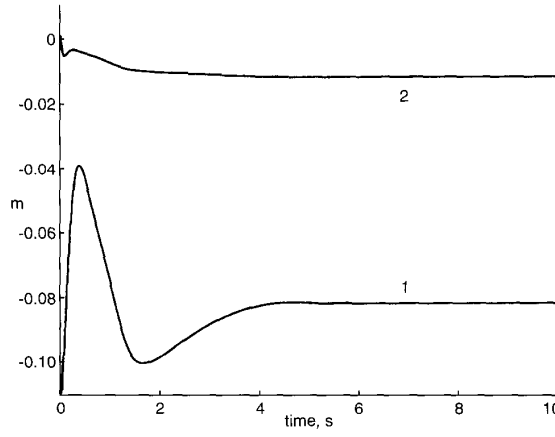


Fig. 15 Time histories of first link deflections in second case study

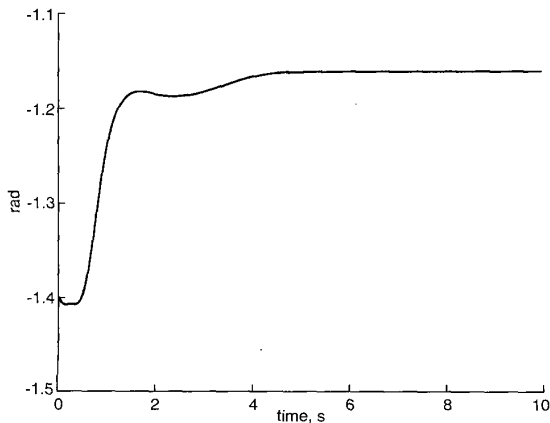


Fig. 13 Time history of first joint angle in second case study

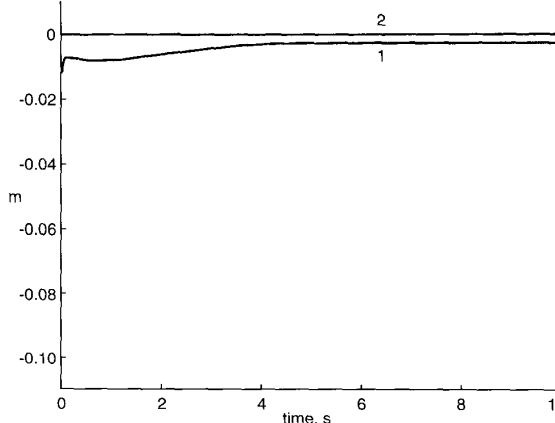


Fig. 16 Time histories of second link deflections in second case study

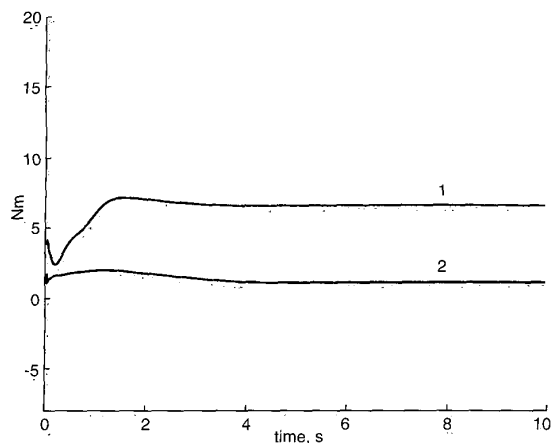


Fig. 17 Time histories of joint torques in second case study

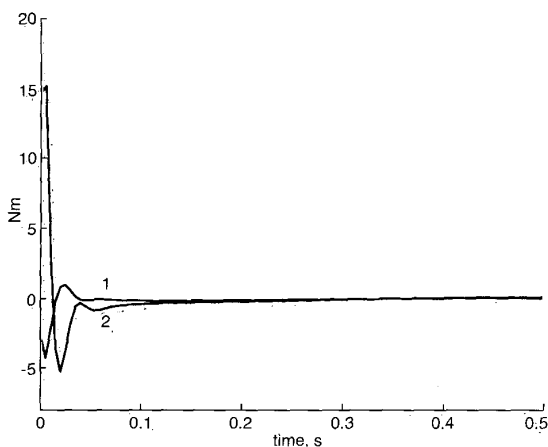


Fig. 18 Time history of fast control in second case study

It is worth pointing out that the simulation of both the slow control laws without the fast control action (eqn. 19) has revealed an unstable behaviour; the results have not been reported for brevity.

7 Conclusions

The problem of force and position control for flexible link manipulators has been considered in this paper. Because of the presence of structural link flexibility, the additional objective of damping the vibrations that are naturally excited during task execution was considered. By using the singular perturbation theory, under the reasonable hypothesis that link stiffness is large, the system has been split into a slow subsystem describing the rigid motion dynamics and a fast subsystem describing the flexible dynamics. Then a force and position parallel control has been adopted for the slow subsystem, while a fast action has been designed for vibration damping. Simulation results have confirmed the feasibility of the proposed approach.

8 Acknowledgments

This work was supported in part by *MURST* and in part by *ASI*.

9 References

- BOOK, W.J.: 'Controlled motion in an elastic world', *ASME J. Dyn. Syst., Meas. Control*, 1993, **115**, pp. 252-261
- MEIROVITCH, L.: 'Analytical methods in vibrations' (Macmillan, New York, NY, 1967)
- BOOK, W.J.: 'Recursive Lagrangian dynamics of flexible manipulator arms', *Int. J. Robotics Res.*, 1984, **3**, (3), pp. 87-101
- CANUDAS DE WIT, C., SICILIANO, B., and BASTIN, G.: 'Theory of robot control' (Springer-Verlag, London, 1996)
- KOKOTOVIC, P., KHALIL, H.K., and O'REILLY, J.: 'Singular perturbation methods in control: analysis and design' (Academic Press, New York, 1986)
- SICILIANO, B., and BOOK, W.J.: 'A singular perturbation approach to control of lightweight flexible manipulators', *Int. J. Robotics Res.*, 1988, **7**, (4), pp. 79-90
- FRASER, A.R., and DANIEL, R.W.: 'Perturbation techniques for flexible manipulators' (Kluwer Academic Publishers, Boston, MA, 1991)
- SICILIANO, B., PRASAD, J.V.R., and CALISE, A.J.: 'Output feedback two-time scale control of multi-link flexible arms', *ASME J. Dyn. Syst., Meas. Control*, 1992, **114**, pp. 70-77
- VANDEGRIFT, M.W., LEWIS, F.L., and ZHU, S.Q.: 'Flexible-link robot arm control by a feedback linearization/singular perturbation approach', *J. Robot. Syst.*, 1994, **11**, pp. 591-603
- MOALLEM, M., KHORASANI, K., and PATEL, R.V.: 'An integral manifold approach for tip-position tracking of flexible multi-link manipulators', *IEEE Trans. Robot. Autom.*, 1997, **13**, pp. 823-837
- SICILIANO, B., and VILLANI, L.: 'Robot force control' (Kluwer Academic Publishers, Boston, MA, 1999)
- CHIOU, B.C., and SHAHINPOOR, M.: 'Dynamic stability analysis of a two-link force-controlled flexible manipulator', *ASME J. Dyn. Syst., Meas. Control*, 1990, **112**, pp. 661-666
- MILLS, J.K.: 'Stability and control aspects of flexible link robot manipulators during constrained motion tasks', *J. Robot. Syst.*, 1992, **9**, pp. 933-953
- MATSUNO, F., ASANO, T., and SAKAWA, Y.: 'Modeling and quasi-static hybrid position/force control of constrained planar two-link flexible manipulators', *IEEE Trans. Robot. Autom.*, 1994, **10**, pp. 287-297
- MATSUNO, F., and YAMAMOTO, K.: 'Dynamic hybrid position/force control of a two degree-of-freedom flexible manipulator', *J. Robot. Syst.*, 1994, **11**, pp. 355-366
- HU, F.L., and ULISOY, A.G.: 'Force and motion control of a constrained flexible robot arm', *ASME J. Dynam. Syst., Meas. Control*, 1994, **116**, pp. 336-343
- YANG, J.-H., LIAN, F.-L., and FU, L.-C.: 'Adaptive hybrid position/force control for robot manipulators with compliant links', Proceedings 1995 IEEE International Conference on Robotics and automation, 1995, Nagoya, Japan, pp. 603-608
- LEW, J.Y., and BOOK, W.J.: 'Hybrid control of flexible manipulators with multiple contact', Proceedings of the 1993 IEEE International Conference on Robotics and automation, 1993, Atlanta, GA, **2**, pp. 242-247
- YOSHIKAWA, T., HARADA, K., and MATSUMOTO, A.: 'Hybrid position/force control of flexible-macro/rigid-micro manipulator systems', *IEEE Trans. Robot. Autom.*, 1996, **12**, pp. 633-640
- ROCCO, P., and BOOK, W.J.: 'Modelling for two-time scale force/position control of flexible robots', Proceedings of the 1996 IEEE International Conf. on Robotics and automation, 1996, Minneapolis, MN, pp. 1941-1946
- CHIAVERINI, S., and SCIAVICCO, L.: 'The parallel approach to force/position control of robotic manipulators', *IEEE Trans. Robot. Autom.*, 1993, **9**, pp. 361-373
- CHIAVERINI, S., SICILIANO, B., and VILLANI, L.: 'Force/position regulation of compliant robot manipulators', *IEEE Trans. Autom. Control*, 1994, **39**, pp. 647-652
- RAIBERT, M.H., and CRAIG, J.J.: 'Hybrid position/force control of manipulators', *ASME J. Dynam. Syst., Meas. Control*, 1981, **103**, pp. 126-133
- YOSHIKAWA, T.: 'Dynamic hybrid position/force control of robot manipulators: description of hand constraints and calculation of joint driving force', *IEEE J. Robot. Autom.*, 1987, **3**, pp. 386-392
- DE LUCA, A., and SICILIANO, B.: 'Closed-form dynamic model of planar multilink lightweight robots', *IEEE Trans. Syst. Man. Cybern.*, 1991, **21**, pp. 826-839
- SICILIANO, B.: 'Closed-loop inverse kinematics algorithms for constrained flexible manipulators under gravity', *J. Robot. Syst.*, 1999, **16**, pp. 353-362